Universal Journal of Physics and Application 11(3): 91-96, 2017 http://www.hrpub.org
DOI: 10.13189/ujpa.2017.110304

Optical and Electrical Properties of Antimony and Fluorine Doped Tin Oxide Thin Films

Saw Lin Oo[1], Zayar Thu[2], Than Zaw Oo[3], Pho Kaung[4,*]

[1]Department of Physics, University of East Yangon, Myanmar
[2]Department of Physics, Maubin University, Myanmar
[3]Department of Physics, Panglong University, Myanmar
[4]University of Yangon, Myanmar

Abstract The Sb:F:SnO_2 layers (AR) were prepared by spray pyrolysis method. The anti-reflective layers (AR) heat-treated at 500°C for 30 min (solution amount 20 cc and 25 cc) have shown an improved crystallinity with crystallite size of 38-39 nm, high optical transmission of around 70 % at 450 nm. Incorporation of anti-reflective layer at cathode interface of SiO_2/Si(N) devices increased the power conversion efficiency from 1.2% to 2.7% which is mainly contributed from photocurrent enhancement. The enhanced efficiency mainly contributed to the increase in J_{sc}. It is attributed to enhanced light absorption and better charge transport in the SiO_2/Si (N) device with Sb:F:SnO_2 AR layer. Results of optical and electrical studies show that the films are well suited for thin film solar cell as a window layer.

Keywords Anti-reflective Layer (AR), Antimony and Fluorine Doped Tin Oxide (Sb:F:SnO_2)

1. Introduction

In order to enhance the performance of a solar cell, it needs to reduce the reflection loss from the surface of the cell [1]. A flexible optical design for light collection is vital in achieving high performance solar cells. An ideal anti-reflective (AR) structure leads to zero reflection loss on solar cell surfaces over an extended solar spectral range for all angles of incidence. Thus, the perfect anti-reflective structure has been a subject of intensive research in thin film optics and most importantly, for solar cell applications [2].The interfacial layer in a Schottky barrier solar cell plays an important role in determining the short circuit current, open circuit voltage, fill factor and efficiency of the cell. The effects of interfacial oxide layer thickness on the open circuit voltage and efficiency of the cells have been increased [3]. Aluminum (Al) and Silver (Ag) metal layers were used in place of the counter and back electrodes [1, 4]. Among these, Sb:F:SnO_2 is chosen as an anti-reflective (AR) layer because of its high electrical conductivity and its transparency in the visible and infrared light [5, 6]. Further, its refractive index lies in between 1.7 and 2.0 and hence it can be used as an antireflection (AR) coating [7]. In addition, Sb:F:SnO_2 layer provides both high optical transmittance and high electrical conductivity simultaneously. The sol-gel processing exhibits good uniformity and better-controlled composition for thin film deposition by the spinning or spray pyrolysis method [6,8]. In this study, an attempt is made to find the effect of different layers on its optical and electrical properties by simultaneously doping antimony and fluorine. In addition, the effect of an anti-reflective layer on the photovoltaic efficiency of SiO_2/Si solar cells is also highlighted.

2. Materials and Methods

2.1. Substrate Cleaning

The substrate cleaning is very important in the deposition of thin films. The substrates used in this work were phosphor doped N-type silicon with the resistivity value of 0.01~10Ωcm and orientation of (100) plane. The Si substrate was cut into the dimension of 1" x 1". Firstly the substrate was cleaned with HF: H_2O (1:5) for 10 minutes to remove native oxide and immersed in acetone for 10 minutes. Then the substrate was immersed in methyl alcohol for 10 minutes to remove the impurities. After that, it was rinsed with deionized water (DI water) for a few minutes and dried with nitrogen blow at room temperature [9,10].

2.2 Deposition of Sb:F:SnO_2 Film

The Sb:F:SnO_2 thin films were prepared as per synthesis route shown in Figure 1. The $SnCl_4.5H_2O$ (98 % purity), $SbCl_3$ (99 % purity), and NH_4F (98 % purity) were used as

precursors. $SnCl_4.5H_2O$ (10g) was dissolved in ethanol (80ml) at room temperature under stirring. On the other hand, 2g of NH_4F was dissolved in 10ml deionized water and 3g of antimony trichloride ($SbCl_3$) was separately dissolved in ethanol (20 ml). Over a period of exactly 10 minutes, NH_4F solution and $SbCl_3$ solution were added to the $SnCl_4.5H_2O$ solution. The mixture solution was continuously stirred for 12 hours at 60°C by solochemical method. Solution became transparent and filtered by 0.45 μm pole size filters. The clear solution of 20 cc, 25 cc and 30 cc were used to make anti-reflective ($Sb:F:SnO_2$) layers with working distance of about 20 cm and angle of 90° by spray pyrolysis method. The substrates temperature was kept at 500°C and monitored by digital temperature controller. Finally, the films were annealed at 500°C for 30 minutes and measured for their optical and electrical properties [1, 11].

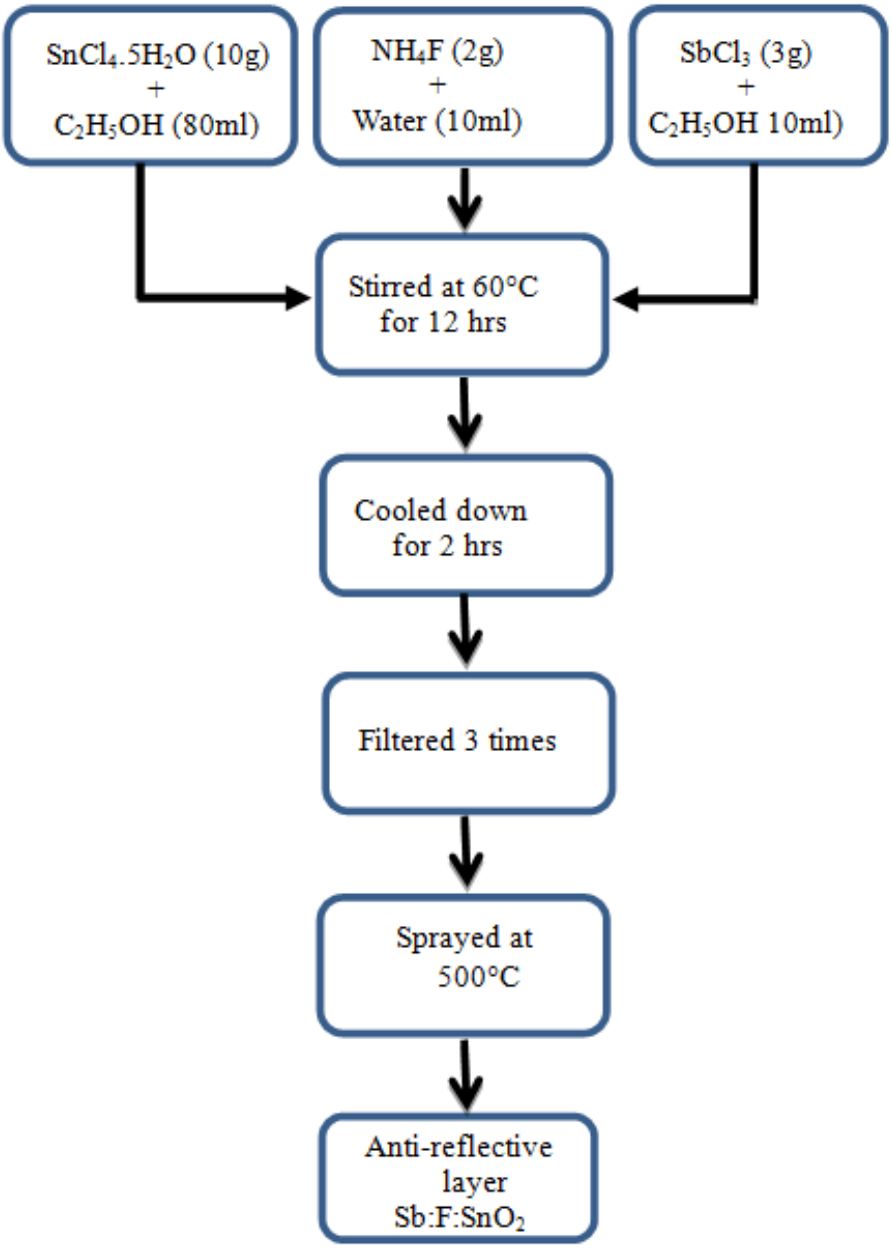

Figure 1. The synthesis route of anti-reflective layer

3. Results and Discussion

3.1 Structural Properties of Sb:F:SnO_2 Films

Structural studies of Sb:F:SnO_2 films with solution amount of 20 cc, 25 cc and 30 cc heat-treated at 500°C for 30 minutes were done using X-ray diffraction (XRD) technique. The crystalline sharp peaks in the diffraction patterns were identified by using the International Centre for Diffraction Data (ICDD). The crystalline size was calculated by using Scherer's equation; $D = (k\lambda)/(B \cos\theta)$ where, B is the peak width measured at half intensity (radian), λ is the wavelength measured in Å, k is the particle shape factor or Scherer constant (k = 0.9) and D is the diameter of the crystallites (Å).

The XRD spectra for Sb:F:SnO_2 films with 20 cc, 25 cc and 30 cc are depicted in Figure 2. XRD diffraction peaks belonging to (110), (101), (200), (211) and (301) were observed in all the Sb:F:SnO_2 films which are well matched with the powder diffraction data of 77-0447> Cassiterite, syn-SnO_2, 88-2348> Sn.918Sb.109O_2- Tin Antimony Oxide and 70-0164>SnF_2-Tin Fluoride. For the samples using 20 cc and 25 cc solution amount, the diffraction peaks were pronounced sharper indicating that the crystallinity of Sb:F:SnO_2 was improved at this processing condition. The average crystallite sizes estimated by using Scherer's equation were found to be 38.5 nm, 39.3 nm and 50.9 nm respectively for Sb:F:SnO_2 (20 cc, 25 cc and 30 cc). The Sb:F:SnO_2 has tetragonal structure with a-axis value of 4.7441 Å and c-axis value of 3.1959 Å..

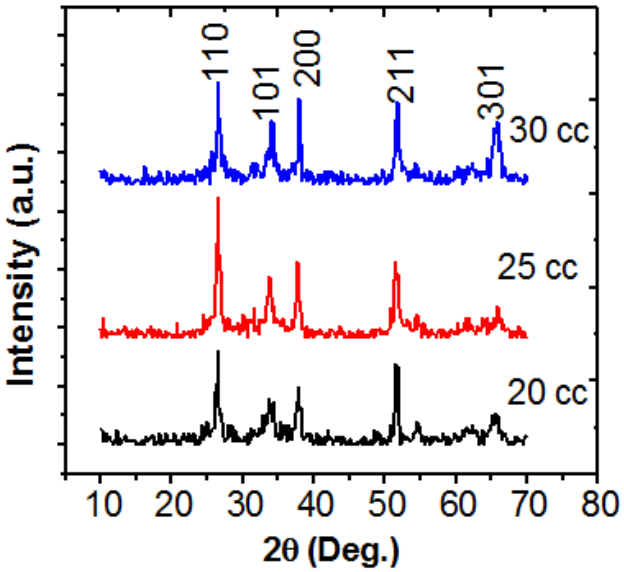

Figure 2. The XRD spectra for Sb:F:SnO_2 films using different solution amounts (20cc, 25 cc and 30 cc).

3.2 Surface Morphology of Sb:F:SnO_2 Films

Surface morphology of Sb:F:SnO_2 were examined by scanning electron microscopy (SEM). Figure 3 shows the SEM images of Sb:F:SnO_2 films (solution amount 30 cc). It is observed that the Sb:F:SnO_2 films were fully covered on the substrate and the particle-like features with submicron size ranging from 0.2 μm to 0.5 μm were mostly found on the film surface.

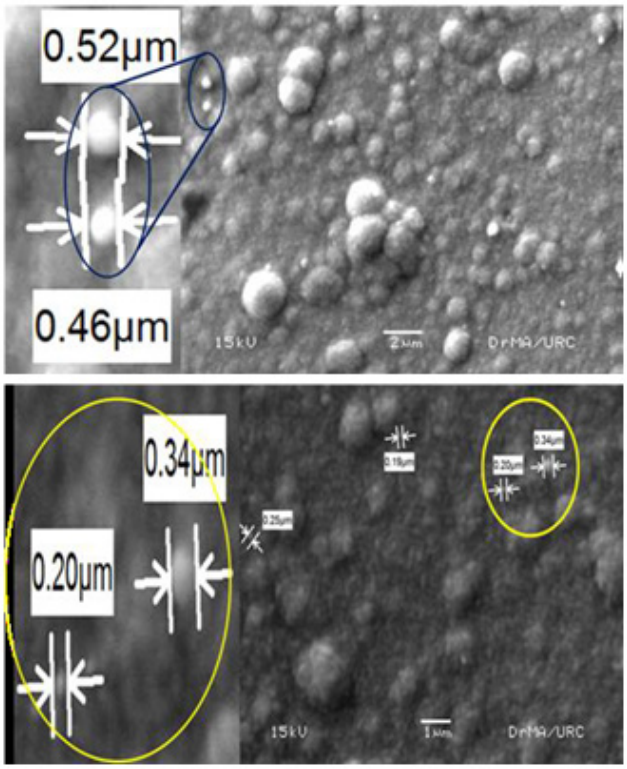

Figure 3. The SEM micrographs of Sb:F:SnO_2 films prepared from solution amount of 25 cc. Magnification: 5500 x (upper) and 10000x (lower)

3.3 Optical Properties

The optical transmission spectra of Sb:F:SnO_2 films using solution amount of 20 cc, 25 cc and 30 cc were recorded in the wavelength of 300 to 800 nm using Shimadzu UV-1800 spectrophotometer. The transmission spectra of SnO_2:F:Sb layers were shown in Figure 4-a. The transmittance value of 40% to 70% was found in the visible region of 400-700 nm. As clearly seen, the optical transmittance decreased (absorption increased) upon increasing solution amount which is ascribed to thicker film formation with higher solution amount. The thickness of the films was determined by surface profiler (Tencor Alpha step IQ) and the values are listed in Table 1. In addition, the optical band gaps of SnO_2:F:Sb anti-reflective layers were estimated from the plot of $(\alpha h\nu)^2$ versus hν as shown in Figure 4-b. The extrapolation of the linear region of the plot toward x-axis provides the optical band gap energy value. The band gap energy was found to be 3.0 eV, 3.4 eV and 3.8 eV for 20 cc, 25 cc and 30 cc respectively. Higher optical transmission and wider band gap energy are preferred for interlayer (anti-reflective layer) in solar cells.

The refractive index (n) of each and every layer in multilayer solar cells is a key parameter which can determine the optical electric field distribution and absorption of the solar cell. The refractive index of Sb:F:SnO_2 layer (20 cc)

was determined by spectroscopic ellipsometer (J.A. Woolam Co. Inc M-44). Figure 4-c depicts the plot of refractive index versus wavelength. The incident angle of 75.2° was used and the data was fit using Cauchy model. The refractive index of Sb:F:SnO_2 layer was found to be 1.8 corresponding to the wavelength 580 nm for all SnO_2:F:Sb films.

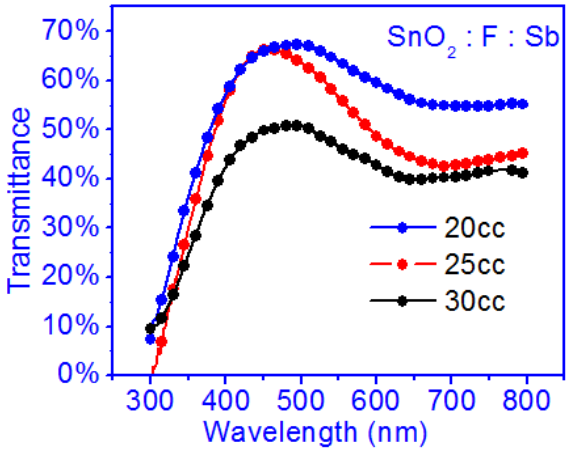

(a)

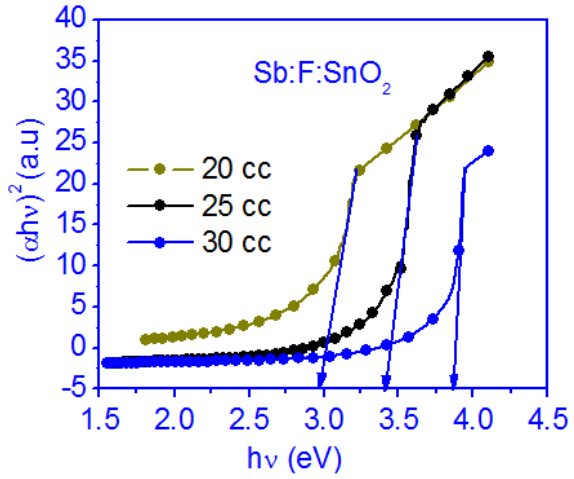

(b)

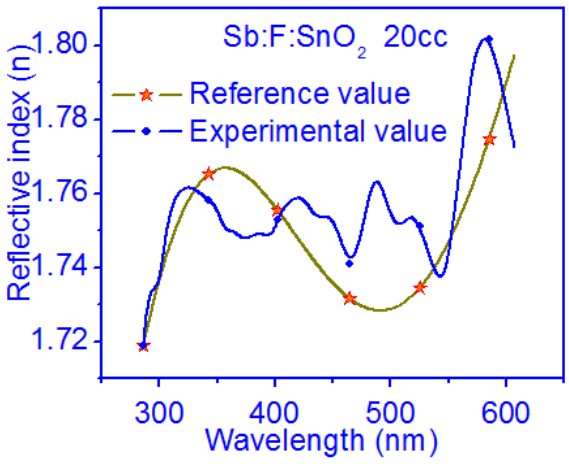

(c)

Figure 4. (a) Optical transmission spectra, (b) plot of $(\alpha h\nu)^2$ versus hν for Sb:F:SnO_2 films (solution amount of 20 cc, 25 cc and 30 cc) and (c) plot of refractive index vs. wavelength for Sb:F:SnO_2 film (20 cc).

Table 1. The refractive index, film thickness and optical band gap energy of Sb:F:SnO_2 films.

Volume of Spray solution (cc)	Refractive index	Thickness (nm)	Eg (eV)	Resistance (Ω)
20	1.8	63.9	3.0	85.6
25	1.8	103.2	3.4	45.6
30	1.8	122.9	3.8	30.2

3.4. Electrical Properties of Sb:F:SnO_2 Films

Electrical conductivity (mobility) of anti-reflective layer is also important to be measured since it would determine the chare transport. The electrical resistance values of Sb:F:SnO_2 films were measured by using digital multimeter and are listed in Table 1. The electrical resistance increased with increasing film thickness.

3.5. Impact of Sb:F:SnO_2 Anti-reflective Layers on Photocurrent Generation

The Sb:F:SnO_2 anti-reflective layer has been integrated at the cathode interface of the Si/SiO_2 photovoltaic device. Figure 5 shows the schematic diagram of SiO_2/Si (N) device with and without anti-refractive layer together with their photographs. Figure 6 shows the current-voltage (I-V) characteristics of SiO_2/Si(N) photovoltaic device with and without anti-reflective layer. The critical parameters for the device with and without anti-reflective layer are listed in Table (2).

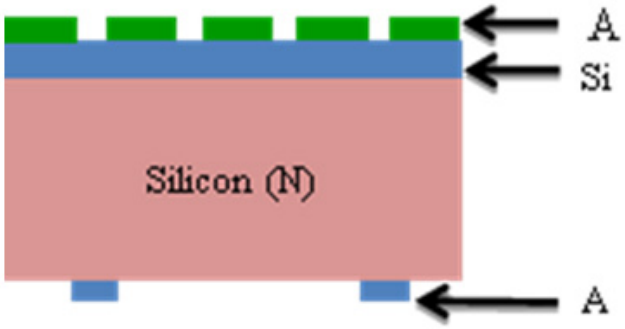

(a)

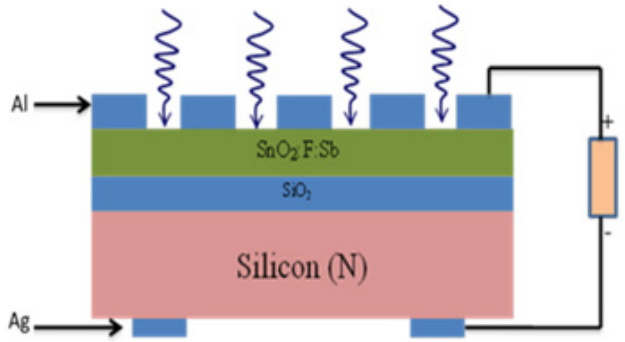

(b)

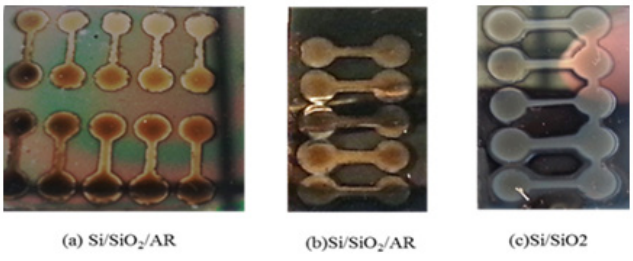

(c)

Figure 5. Schematic diagram of SiO_2/Si(N) device (a) without anti-reflective layer and (b) with anti-reflective layer and (c) Photographs of the SiO_2/Si(N) devices.

The reference device without anti-reflective layer provided the short-circuit current density (J_{sc}) of 71.28mA/cm^2, open circuit voltage (V_{oc}) of 4.4 mV and fill factor (FF) of 0.38 yield power conversion efficiency (PCE) of 1.2% under light source 100 mWcm^{-2}. Upon integrating anti-reflective layer (Sb:F:SnO_2 20 cc and 25 cc) at the cathode interface of the device, the J_{sc} increased from 71.28mA/cm^2 to 81.14 mA/cm^2 and 90 mA/cm^2 and FF from 0.38 to 0.56 and 0.60, V_{oc} from 4.4 mV to 4.7 mV and 5.0mV and power conversion efficiency increased from 1.20 % to 2.15 % and 2.70 % respectively for the SiO_2/Si (N) device with Sb:F:SnO_2 AR layer (20 cc ad 25 cc). The enhanced efficiency mainly contributed to the increase in J_{sc}. The increased J_{sc} is attributed to enhanced light absorption and better charge transport in the SiO_2/Si (N) device with Sb:F:SnO_2 AR layer.

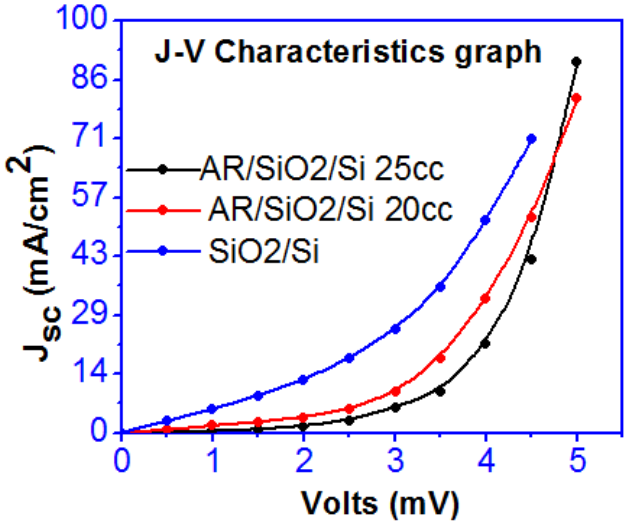

Figure 6. I-V characteristics of SiO_2/Si (N) photovoltaic device with and without anti-reflective layers

Table 2. The critical device parameters of SiO_2/Si (N) device with and without Anti-reflective (AR) layer.

Devices	J_{sc} (mAcm^{-2})	FF	V_{oc} (mV)	PCE (%)
Without AR layer	71.28	0.38	4.4	1.20
With AR layer (20cc)	81.14	0.56	4.7	2.15
With AR layer (25cc)	90.00	0.60	5.0	2.70

4. Conclusions

The Sb:F:SnO_2 layers (AR) were prepared by spray pyrolysis method. The anti-reflective layers (AR) (solution amount 20 cc and 25 cc) have shown an improved crystallinity with crystallite size of 38-39 nm, high optical transmission of 70% at 450 nm. Incorporation of anti-reflective layer at cathode interface of SiO_2/Si(N) devices increased the power conversion efficiency from 1.2% to 2.7% which is mainly contributed from photocurrent enhancement. The enhanced efficiency mainly contributed to the increase in J_{sc}. It is attributed to enhanced light absorption and better charge transport in the SiO_2/Si(N) device with Sb:F:SnO_2 AR layer. Results of optical and electrical properties show that the films are well suited for window layer on thin films solar cells.

Acknowledgements

The author (SLO) thanks Organizing Committee of the 4th International Conference on Applied Engineering Physics for their kind invitation to present this research work.

REFERENCES

[1] D. Hocine, M.S. Belkaïd, and K. Lagha, "Influence of interfacial oxide layer thickness on conversion efficiency of SnO2/SiO2/Si (N) Solar Cells," *Rev. des Energies Renouvelables*, vol. 11(3), pp. 379-384, 2008.

[2] L.Chinnappa, K. Ravichandran and B. Sakthivel,"Investigation on Doubly Doped (Fluorine + Antimony) Tin Oxide Films Deposited by a Simplified Spray Pyrolysis Technique" *Pro. Indian Natn. Sci. Acad.* vol.79(3), pp. 409-415, 2013.

[3] D. Hocine and M.S. Belkaid, "Effects of interfacial oxide layer thickness and interface states on conversion efficiency of SnO_2/SiO_2/Si(N) solar cells" *RE&PQJ* vol. 1(6), pp. 170–174, 2008.

[4] M.A. Muhsien, E.T. Salem, and I.R. Agool, "Preparation and characterization of (Au/n-SnO_2/SiO_2/Si/Al) MIS Device for Optoelectronic Application" *Int. J. Opt.* vol. 2013 (756402), pp. 1-9, 2013.

[5] A.R. Babar, S.S. Shinde, A.V. Moholkar, C.H. Bhosale, J.H. Kim, and K.Y. Rajpure, "Sensing properties of sprayed antimony doped tin oxide thin films: Solution molarity" *J. Alloys Compd.*, vol. 509(6), pp. 3108–3115, 2011.

[6] Z.Y. Banyamin, P.J. Kelly, G. West, and J. Boardman, "Electrical and Optical Properties of Fluorine Doped Tin Oxide Thin Films Prepared by Magnetron Sputtering," *Coatings*, vol. 4, pp. 732–746, 2014.

[7] S. Abdullahi, A.U. Moreh, B. Hamza, U. Sadiya, Z. Abdullahi, M.A. Wara, H. Kamaluddeen, M.A. Kebbe and U.F. Monsurat, "Optical Characterization of Fluorine doped Tin Oxide (FTO) thin films deposited by spray pyrolysis technique and annealed

under Nitrogen atmosphere," *International Journal of Innovation and Applied Studies*, vol. 9(2) pp. 947–955, 2014.

[8] T. R. Giraldi, M. T. Escote, A. P. Maciel, E. Longo, E. R. Leite, and J. A. Varela, "Transport and sensors properties of nanostructured antimony-doped tin oxide films," *Thin Solid Films*, vol. 515(4), pp. 2678–2685, 2006.

[9] Dr. Khalid K. Mohammed, Ghassan H. Shakoory, and Ziyad J. Jerjees, "Study and Fabrication of High Efficiency Indium Doped SnO_2/SiO_2/n– Si Solar Cells" *Al-Rafidain Engineering*, vol.20 (3), pp. 1– 43, 2012.

[10] Aqel Mashot Jafar, Kiffah Al-Amara, Farhan Lafta Rashid and Ibrahim Kaittan Fayyadh, "Fabrication and Characterization of Fluorine-Doped Tin Oxide Transparent Conductive Nano-Films"*International Journal of Innovative Research in Engineering & Science*, ISSN 2319-5665, vol. 6 (2), pp.49–58, 2013.

[11] Li Chen, Hongjun Yang, Men Tao and Weidong Zhou, "Microstructured anti-reflection surface design for the omni-directional solar cells" *Proc. of SPIE* vol. 7046 704608-1, 2008.